

Scientific paper

# Synthesis, Spectral, Thermal Analysis, Biological Activity and Kinetic Studies of Copper(II)-Pyridine-2,5-dicarboxylate Complexes with 2-Aminomethylpyridine and 8-Hydroxyquinoline

Alper Tolga Çolak,<sup>1,\*</sup> Ferdağ Çolak,<sup>2</sup> Necip Atar<sup>1</sup>  
and Asım Olgun<sup>1</sup>

<sup>1</sup> Department of Chemistry, Faculty of Arts and Sciences, Dumlupınar University, 43820 Kütahya, Turkey

<sup>2</sup> Department of Biology, Faculty of Arts and Sciences, Dumlupınar University, 43820 Kütahya, Turkey

\* Corresponding author: E-mail: acolak@dumlupinar.edu.tr  
Tel.: +90-2742652051

Received: 05-08-2009

## Abstract

In this work we report the synthesis of two novel square-planar copper(II) complexes, namely, (2-aminomethylpyridinium-pyridinedicarboxylato)copper(II) dihydrate,  $[\text{Cu}(\text{pydc})(2\text{-amp})] \cdot 2\text{H}_2\text{O}$  (**1**) and (8-hydroxyquinolinium-pyridinedicarboxylato)copper(II) hydrate,  $[\text{Cu}(\text{pydc})(8\text{-HQ})] \cdot \text{H}_2\text{O}$  (**2**) (2-amp = 2-aminomethylpyridine, 8-HQ = 8-hydroxyquinoline,  $\text{H}_2\text{pydc}$  = pyridine-2,5-dicarboxylic acid or isocinchomeric acid) and present the first preliminary study on kinetics and biological activities of copper complexes. The synthesized complexes have been characterized by elemental, spectroscopic (FT-IR, UV and mass spectra), thermal analysis, magnetic and conductivity measurements techniques. Kinetic parameters were obtained for each stage of thermal degradation of the complexes using Coats–Redfern and Horowitz–Metzger methods. Antimicrobial activities of two complexes and two ligands were evaluated using agar diffusion method. Antimicrobial activity of complex **2** was determined with the agar dilution methods. The results were compared with two well known antibiotics, namely, tetracycline and nystatin.

**Keywords:** Pyridine-2,5-dicarboxylato complexes, Copper(II) complexes, Antimicrobial activity, Thermal decomposition, Mass spectrometry

## 1. Introduction

The study of metal complexes has received an extensive interest due to their interesting structural diversity as well as potential applications as functional materials. Pyridinedicarboxylates (pydc) such as 2,3-pydc, 2,4-pydc, 2,5-pydc, 2,6-pydc, 3,4-pydc, 3,5-pydc have been extensively used in the synthesis of these compounds.<sup>1–12</sup> Pyridine-2,5-dicarboxylate (pydc) is an efficient ligand with three coordinating sites. Some polymeric structures of pydc complexes with transition and lanthanide metal atoms have been reported in which pydc ligand has shown not only strong chelating ability, but also bridging tendency to form diversified structures.<sup>13–21</sup> Metal pyridinedicarboxylates have interesting properties in biological

systems and their presence seems to be related with metal transport and cell membrane protection in some microorganisms.<sup>22</sup> Among these metal complexes, copper(II) complexes are of great interest since they possess biological activity in their chelating ability that promote structural activity correlations of complexes. A series of copper(II) complexes with pyridine-2,5-dicarboxylic acid,  $[\text{Cu}(\text{pydc})(\text{H}_2\text{O})]_n$ ,<sup>16</sup>  $[\text{Cu}(\text{pydc})_2\text{Mn}(\text{H}_2\text{O})_2]_x \cdot 4x\text{H}_2\text{O}$ ,<sup>23</sup>  $(\text{Hdma})_2[\text{Cu}(\text{pydc})_2]$ <sup>24</sup> (dma = dimethylamine),  $[\text{Cu-Pb}(\text{pydc})_2]$ ,<sup>25</sup>  $[\text{Cu}(\text{pydc})_2]_n$ ,<sup>26</sup>  $\{[\text{Cu}_3(\text{pydc})_3(\text{H}_2\text{O})_3] \cdot 6\text{H}_2\text{O}\}_n$  and  $\{[\text{Cu}(\text{pydc})(\text{H}_2\text{O})] \cdot 2\text{H}_2\text{O}\}_n$ ,<sup>27</sup>  $\{[\text{Cu}(\text{pydc})_2][\text{Cu}(\text{dpya})_2]$  (dpya = 2,2'-dipyridylamine)<sup>28</sup> were synthesized. Due to their importance in biological processes, synthesis and activity studies of Cu(II) complexes have been the focus from different perspectives. Studies rela-

ted to the thermal decomposition and dehydration kinetics and biological activity of copper complexes will give a new insight for future applications.

Although it is well known that the complexes formed from 2-amp ligand with an N–C–C–N skeleton structure show the potent anti-tumour activity, there are limited studies on the biological activities of these complexes.<sup>29</sup> 8-HQ also has a broad antimicrobial spectrum. It is highly active against some viruses, Gram-positive bacteria, Gram-negative cocci but relatively inactive against Gram-negative rods. 8-HQ and its halogenated derivatives are effective against amoebae, plasmodia and trypanosomes. 8-HQ many of its methyl and halogenated derivatives and its metal chelates are broadly antifungal.<sup>30</sup> Thus, efforts have been made on the synthesis of Cu(II)-(pydc) complexes with 2-amp and 8-HQ ligands. The synthesized complexes have been characterized by elemental analysis, FT-IR and mass spectroscopy, magnetic and conductivity measurements. Thermal decomposition of copper complexes was studied using thermogravimetry (TG) and differential thermal analysis (DTA) techniques and kinetic and thermodynamic parameters have been evaluated. Biological activity of copper complexes was also reported.

## 2. Experimental Analyses

### 2.1. Materials and Measurements

All chemicals and solvents used for the synthesis were of reagent grade. Pyridine-2,5-dicarboxylic acid, 2-aminomethylpyridine, 8-HQ = 8-hydroxyquinoline, C<sub>2</sub>H<sub>5</sub>OH, Cu(CH<sub>3</sub>COO)<sub>2</sub>·H<sub>2</sub>O (Aldrich) were used as received. Elemental analysis (C, H, and N) was performed using a Vario EL III CHNS elemental analyzer. Magnetic susceptibility measurement was performed at room temperature using a Sherwood Scientific MK1 model Gouy magnetic balance. UV-vis spectrum was obtained in the water solution (10<sup>-3</sup> mol/L) of the complex with a Shimadzu Pharmaspec UV-1700 spectrometer in the range of 1000–190 nm. FT-IR spectrum was recorded in the 4000–400 cm<sup>-1</sup> region with a Bruker Optics, Vertex 70 FT-IR spectrometer using KBr pellet. Diamond TG/DTA thermal analyzer was used to record simultaneous TG, DTG and DTA curves in the static air atmosphere at a heating rate of 1 °C min<sup>-1</sup> in the temperature range of 35–550 °C using platinum crucibles. The molar conductivities (10<sup>-3</sup> M) were recorded using a WTW model 315i conductivity meter. Mass spectra were obtained on a Thermo Finnigan LCQ Advantage MAX LC/MS/MS spectrometer using ion-trap mass analyzer for ESI source. Finnigan Xcalibur® 1.4 was used to collect and process data. Experimental details of the analyses were done at 319.90 and 323.00 °C for capillary temperature and 33.37 V for capillary voltage. Sheath Gas and Aux/Sweep Gas flow rate were 39.50 and 19.60, respectively.

### 2.2. Syntheses of 1 and 2

A solution of pyridine-2,5-dicarboxylic acid (1 mmol, 0.167 g) in EtOH–H<sub>2</sub>O (1:1; 30 mL) was added drop wise to a solution of 30 mL Cu(CH<sub>3</sub>COO)<sub>2</sub>·H<sub>2</sub>O in water (1 mmol, 0.200 g) at room temperature. A solution in ethanol (30 mL) of 2-aminomethylpyridine (1 mmol, 0.108 g) was added in this solution. After stirring for 2 h at room temperature, the resulting clear blue amorphous solid was observed. The solid precipitated was collected by filtration, washed several times with EtOH and dried on air. In order to synthesize complex with 2, a solution of pyridine-2,5-dicarboxylic acid (1 mmol, 0.167 g) in EtOH–H<sub>2</sub>O (1:1; 30 mL) was added drop wise to an aqueous solution (30 mL) of Cu(CH<sub>3</sub>COO)<sub>2</sub>·H<sub>2</sub>O (1 mmol, 0.200 g) at 50 °C. Then, a solution of 40 mL 8-hydroxyquinoline (1 mmol, 0.145 g) in ethanol was added in this solution. After 1 h stirring at room temperature, the resulting green amorphous solid was observed. The solid precipitated was collected by filtration, washed several times with EtOH and dried on air. *Analytical Data:* C<sub>13</sub>H<sub>15</sub>CuN<sub>3</sub>O<sub>6</sub> for 1 (372.82 g/mol) calcd. C 41.88, H 4.06, N 11.27, found C 42.03, H 4.04, N 11.22, yield 61%, C<sub>16</sub>H<sub>12</sub>CuN<sub>2</sub>O<sub>6</sub> for 2 (391.82 g/mol) calcd. C 49.05, H 3.09, N 7.15, found C 49.40, H 3.15, N 7.11, yield 69%.

### 2.3. Antimicrobial Activity Assay

#### 2.3.1. Test Microorganisms

In this study, total of 11 microbial species including 8 bacteria, 2 yeasts and 1 mould were used as test organisms. The antimicrobial activity of the synthesized compounds are evaluated against Gram-positive (*Bacillus cereus* NRRL 3711, *Staphylococcus aureus* ATCC 25923, *Staphylococcus epidermidis* ATCC 12228, *Neisseria canis*) and Gram-negative (*Escherichia coli* ATCC 25922, *Proteus vulgaris* NRRL-B-123, *Enterobacter aerogenes* NRRL B-3567, *Pseudomonas aeruginosa* ATCC 27853) bacteria, yeast and mould cultures (*Candida albicans* ATCC 10231, *Rhodotorula rubra*, *Aspergillus niger* ATCC 10949). All bacteria strains were stored at –20 °C in the appropriate medium containing 10% glycerol. Fungal cultures of test organisms were maintained on nutrient slants at 4 °C. Cultures from solid medium were sub-cultivated in liquid media, incubated and used as the source of inoculums for each experiment. The disc diffusion method was employed for the determination of the antimicrobial activity of the synthesized compounds.<sup>31</sup> In determination of the minimal inhibitory concentration (MIC) of the synthesised compounds, the agar dilution method was employed.<sup>32,33</sup> The MIC was determined as the lowest concentration of the compound inhibiting the visible growth of each organism on the agar plate. The presence of one or two colonies was disregarded. Each assay in this experiment was repeated three times.

### 3. Results and Discussion

#### 3. 1. FT-IR Spectrum

In the absence of a powerful technique such as X-ray crystallography, FT-IR spectra has proven to be the most suitable technique to give sufficient information to explain the way of bonding of the ligands to the metal ions. The main IR bands with their tentative assignments are summarized in Table 1. The characteristic IR band observed for **1** at 3339 cm<sup>-1</sup> is attributed to the  $\nu(\text{OH})$  vibrations of water molecules.<sup>34–36</sup> The absorption bands at 3216 and 3252 cm<sup>-1</sup> are attributed to the  $\nu(\text{NH}_2)$  vibrations of 2-amp molecule. The strong absorption band at 1741 cm<sup>-1</sup> is due to uncoordinated COO<sup>-</sup> stretching band. The band appearing in the 1435–1377 cm<sup>-1</sup> region can be assigned to symmetric stretching vibration of the coordinated carboxylates and the bands in the 1644–1589 cm<sup>-1</sup> region are ascribed to the  $\nu_{\text{OCOasym}}$ .<sup>37</sup> The absorption band at 1604 cm<sup>-1</sup> is due to  $\nu(\text{C}=\text{C}) + \nu(\text{C}=\text{N})$  vibration of pydc and 2-amp in **1**. The strong and broad absorption band at 3362 cm<sup>-1</sup> is reflected on  $\nu(\text{OH})$  vibrations of water and 8-HQ molecules in **2**. The strong absorption band at 1710 cm<sup>-1</sup> is due to uncoordinated COO<sup>-</sup> stretching band in **2**. The infrared spectra of **2** contain prominent  $\nu_{\text{OCOasym}}$  and  $\nu_{\text{OCOsym}}$  stretching bonds around 1604–1598 cm<sup>-1</sup> and 1392–1373 cm<sup>-1</sup>, respectively.<sup>37</sup> The absorption band at 1575 cm<sup>-1</sup> is attributed to the  $\nu(\text{C}=\text{C}) + \nu(\text{C}=\text{N})$  vibration of pydc and 8-HQ in **2**. Although stretching bands of hydrogen bonded carboxylic groups  $\nu(\text{OH})_{\text{acid}}$  appear within the range of 2350 cm<sup>-1</sup> in free H<sub>2</sub>pydc acid,<sup>38</sup> this band does not appear in the complexes and a new carboxylate band  $\nu_{\text{OCOsym}}$  appeared in the region 1435–1377 cm<sup>-1</sup> for **1** and 1392–1373 cm<sup>-1</sup> for **2** indicating that the carboxylic group of H<sub>2</sub>pydc participate in the coordination with the copper(II) ion through deprotonation. In the far IR spectra, the band observed for two complexes at 526–515 cm<sup>-1</sup> (Cu–O) and 416 and 426 cm<sup>-1</sup> (Cu–N) provide conclusive evidence concerning the bonding between nitrogen and oxygen to the copper ions. Our results are in accordance with the studies done by groups of Min,<sup>16</sup> Patrick<sup>23</sup> and Chuang.<sup>27</sup>

#### 3. 2. Electronic Spectrum, Magnetic Study, Molar Conductance and Mass Spectra

The spectroscopic data of the pyridine-2,5-dicarboxylic acid complexes have been obtained in DMSO solutions. In the case of square planar copper complexes, three allowed transitions are expected in the visible region, but often these theoretical expectations are overlooked in practice, and these bands usually appear overlapped due to the very small energy difference between d levels. The molecule reveals  $\pi \rightarrow \pi^*$  and  $n \rightarrow \pi^*$  transition bands in the region 216 nm ( $\epsilon = 114 \text{ M}^{-1} \text{ cm}^{-1}$ ), 220 nm ( $\epsilon = 501 \text{ M}^{-1} \text{ cm}^{-1}$ ) and 260 nm ( $\epsilon = 5312 \text{ M}^{-1} \text{ cm}^{-1}$ ) for **1** and 258 nm ( $\epsilon = 5113 \text{ M}^{-1} \text{ cm}^{-1}$ ), 332 nm ( $\epsilon = 1297 \text{ M}^{-1} \text{ cm}^{-1}$ ) and 401 nm ( $\epsilon = 1452 \text{ M}^{-1} \text{ cm}^{-1}$ ) for **2**. Complex **1** shows a band at 603 nm ( $\epsilon = 93 \text{ M}^{-1} \text{ cm}^{-1}$ ) due to  ${}^2\text{B}_{1g} \rightarrow {}^2\text{E}_g$  transition, while complex **2** shows a band at 670 nm ( $\epsilon = 50 \text{ M}^{-1} \text{ cm}^{-1}$ ) assigned to the envelope of  ${}^2\text{B}_{1g} \rightarrow {}^2\text{B}_{2g}$  transitions suggesting square planar structure of Cu(II) complexes.<sup>39</sup> Magnetic moment values for **1** and **2** at room temperature were 1.74 and 1.64 B.M. respectively. These values are close to the spin-only value for an unpaired spin (~1.73 B.M.). The complexes are soluble in DMF and DMSO, but insoluble in EtOH, MeOH, CHCl<sub>3</sub> and CH<sub>2</sub>Cl<sub>2</sub>. The compounds are very stable solids at room temperature without decomposition. The molar conductivity values for **1** and **2** in DMF ( $1.0 \times 10^{-3} \text{ M}$ ) were in the range of 9.9 and 12.8  $\Omega^{-1} \text{ cm}^2 \text{ mol}^{-1}$ . The observed molar conductance of the complexes at room temperature is consistent with the non-electrolytic nature of the complexes due to no counter ions in the proposed structures of complexes **1** and **2**.<sup>40</sup>

Mass spectra of [Cu(pydc)(2-amp)] · 2H<sub>2</sub>O and [Cu(pydc)(8-HQ)] · H<sub>2</sub>O are given in Fig. 1 and 2, respectively. In the mass spectrum of **1**, the peak observed at  $m/z$  337 possibly corresponds to the molecule produced by the loss of water molecules in the ionization process. The peak [Cu(py)(CO<sub>2</sub>)(2-amp)]<sup>+</sup> observed at  $m/z$  293.16 (7.17% intensity, calcd: 293.79) results in the release of CO<sub>2</sub> from the molecular ion. Other important peak observed at  $m/z$  278.21 (24.87% intensity, calcd: 278.77) can be

Table 1. FT-IR spectroscopic data of **1** and **2** (cm<sup>-1</sup>)\*

Assignment	<b>1</b>	<b>2</b>	Na <sub>2</sub> (pydc)·nH <sub>2</sub> O
$\nu(\text{OH})$	3339 br	3362 s, br	–
$\nu(\text{NH}_2)$	3216 s 3252 s	–	–
$\nu(\text{C}-\text{H})$	3075 w	3086 w	3091 w
$\nu_{\text{uncoord}}(\text{COO}^-)$	1741 vs	1710 vs	–
$\nu_{\text{as}}(\text{COO})$	1644 vs – 1589 vs	1604 vs – 1598 s	1604 s
$\nu(\text{C}=\text{C}) + (\text{C}=\text{N})$	1604 s	1575 s	–
$\nu_{\text{s}}(\text{COO})$	1435 vs – 1377 vs	1392 vs – 1373s	1402 s
$\nu(\text{C}-\text{O})$	1347 vs, 1287 s, 1056 s	1371 vs, 1260s, 1046 s	1354 s
CuO	526 w	515 w	–
CuN	416 w	426 w	–

\* Abbreviations: w – weak; m – medium; s – strong; vs – very strong, b – broad.

attributed to the fragmentation of  $-\text{NH}_2$  from the  $[\text{Cu}(\text{py})(\text{CO}_2)(2\text{-amp})]^+$ . The fragments observed at  $m/z$  171.21 (9.87% intensity, calcd: 171.66), and  $m/z$  107.12 (9.60% intensity, calcd: 107.13) may be assigned to the  $[\text{Cu}(\text{py})(\text{CO})]^+$  and  $[(\text{py})(\text{CH}_2)(\text{NH})]^+$ , respectively. In the mass spectrum of compound **2** (Fig. 2), the intense peak at  $m/z$  374 corresponds to the loss of a water molecule in the ionization process. The  $[\text{Cu}(\text{pydc})(8\text{-HQ})]^+$  was not stable, thus fragments are not clearly seen in the MS spectrum.

### 3. 3. Thermal and Kinetic Analysis

The thermal analysis curves of  $[\text{Cu}(\text{pydc})(2\text{-amp})] \cdot 2\text{H}_2\text{O}$  are given in Fig. 3. The TG curves indicate three different stages of mass loss. Dehydration of two water molecules takes place in the first stage between 35 and 72 °C with a mass loss of 9.5% ( $\text{DTG}_{\text{max}} = 63.1$  °C, calcd: 9.7%). The second stage involves a significant mass loss extending from 95.1 °C to 278 °C which is thought to have been caused by decomposition of the ligand (2-amp) with a mass loss of 28.1% ( $\text{DTG}_{\text{max}} = 208, 239$  and 270

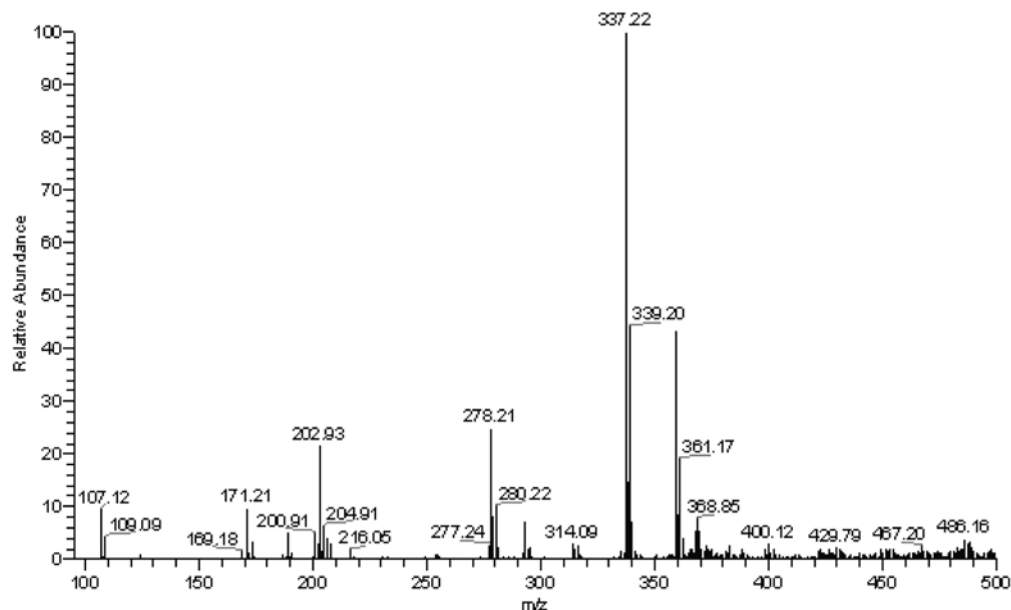


Fig. 1. ESI-Mass spectrum of **1**

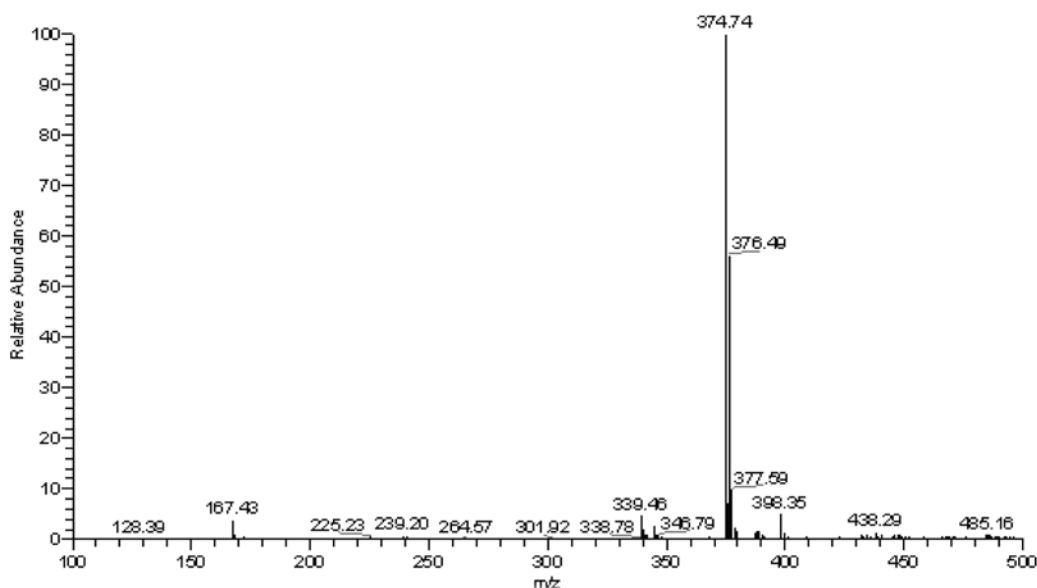


Fig. 2. ESI-Mass spectrum of **2**

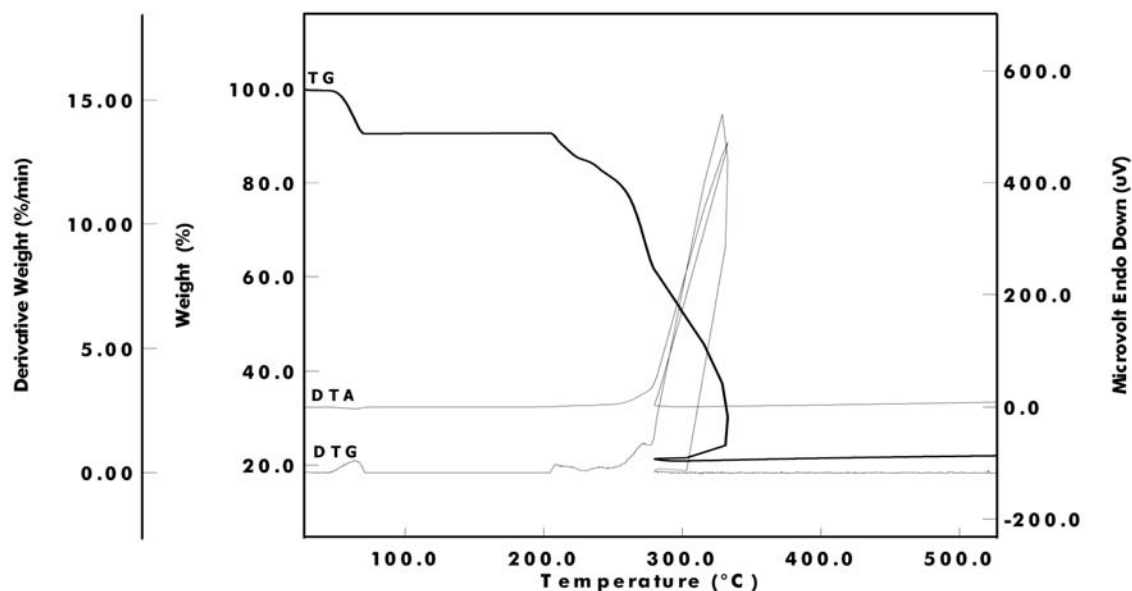


Fig. 3. TG, DTG and DTA curves of 1

°C, calcd: 29.0%). The third stage occurred in the temperature range of 279–333 °C is assigned to the decomposition of the pydc group. The observed mass loss ( $DTG_{max} = 329$  °C, 41.3%) roughly coincides with the theoretical value (44.3%). The differences between theoretical and experimental values can be attributed to the lack of plateau after decomposition of 2-amp. Therefore, it is impossible to define exact decomposition temperature of pydc. The final weight of residue observed as 21.1% (calcd: 21.3) can be attributed to the CuO.

The TG curves of  $[Cu(pydc)(8-HQ)] \cdot H_2O$  complex (Fig. 4) show an initial mass loss in the temperature range of 35–52 °C caused by the decomposition of the crystal water molecule. This is followed by another mass loss in the temperature range of 174–272 °C due to the removal of ligand (8HQ,  $DTG_{max} = 269$  °C, found: 31.2%, calcd: 37.0%). The last stage involves a significant mass loss extending from 272–366 °C with DTG maximum of 297 °C due to the decomposition of pydc. The observed mass loss is 42.1% which is consistent with the theoretical value of

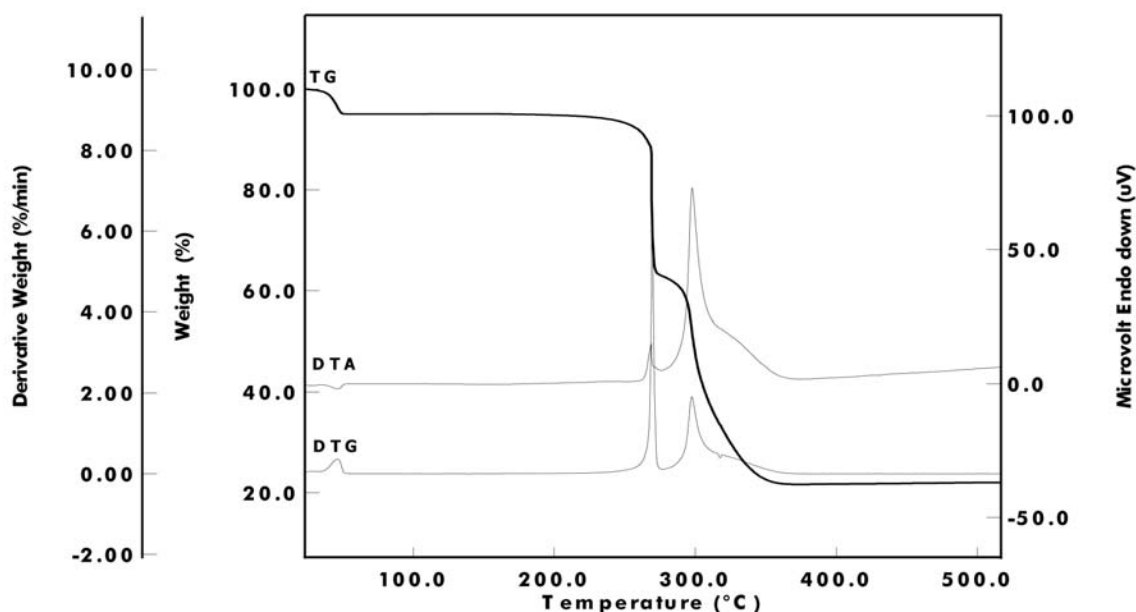


Fig. 4. TG, DTG and DTA curves of 2

42.1%. The end products can be assigned to the CuO by considering calculated mass (20.3%) and observed weights (21.7%). Although, there seems to be a plateau resulting from the decomposition of 8-HQ, it is too short to comment on. The lack of plateau may be attributed to the existence of a ligand in the system. Hence, theoretical values for the ligand are larger than that of the experimental values.

The thermodynamic parameters of decomposition process of complexes, namely, activation energy ( $E_a$ ), enthalpy ( $\Delta H^*$ ), entropy ( $\Delta H^*$ ) and free Gibbs energy change of the decomposition ( $\Delta H^*$ ) were calculated by employing the Horowitz–Metzger<sup>41</sup> and Coats–Redfern<sup>42</sup> relations.

Horowitz–Metzger relation is given as:

$$\ln \left[ \frac{\ln(W_0 - W_t^f)}{W - W_t^f} \right] = \frac{E_a \theta}{RT_s^2}$$

where  $W_0$  is the initial weight of the sample, ( $\Delta H^*$ ) is the final weight of the sample,  $W$  is the weight remaining at a given temperature  $T$ ,  $E_a$  is the activation energy, ( $\Delta H^*$ ),  $T_s$  is the peak temperature of DTG and  $T$  is the temperature corresponding weight loss,  $W$ .

Coats–Redfern relation is as follows:

$$\log \left\{ -\log \left[ \frac{1-\alpha}{T^2} \right] \right\} = \log \left\{ \left( \frac{AR}{aE_a} \right) - \left( \frac{E_a}{2.303RT} \right) \right\}$$

where ( $\Delta H^*$ ) is the fraction of the sample decomposed at time  $T$ ,  $T$  is the derivative peak temperature,  $A$  is frequency factor,  $R$  is the gas constant. A plot of ( $\Delta H^*$ ) versus  $1/T$  gives a slope for the evaluation of activation energy. The kinetic data obtained for the nonisothermal decomposition of complexes are given in Table 2 and Figs. 5 and 6. As seen in Table 2, the apparent activation energy values calculated by Horowitz–Metzger (H–M) and Coats–Redfern (C–R) are close to each other for two copper complexes. Furthermore, the activation energies of the first step in both complexes are almost identical with those of dehydration of other copper complexes.<sup>43,44</sup> In case **1**, a higher value of activation energy is observed in the second stage. The values from two models are in close agreement with each other. In case **2**, we were unable to calculate activation energy of the second stage of degradation primarily due to its complexity. Entropy of activation values are positive for both complexes indicating a variance in structural transformation needed to break bond and form new chemical bonds in the transition state. Therefore, it may be said that the positive values of entropy results from the degradation processes, especially as a consequence of a gaseous product obtained. The suggested structures are illustrated in Fig. 7 and Fig. 8 in the light of these data.

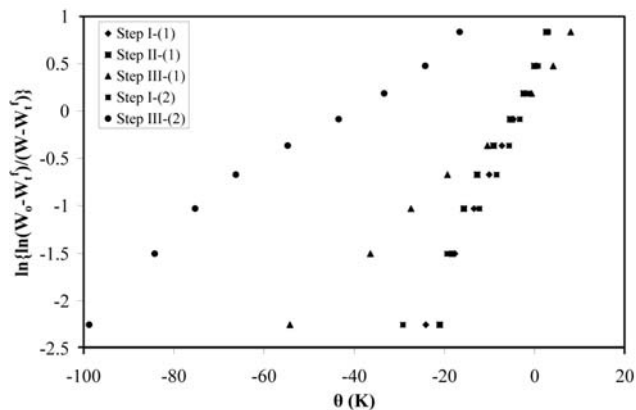


Fig. 5. Typical Horowitz–Metzger plot of the complexes

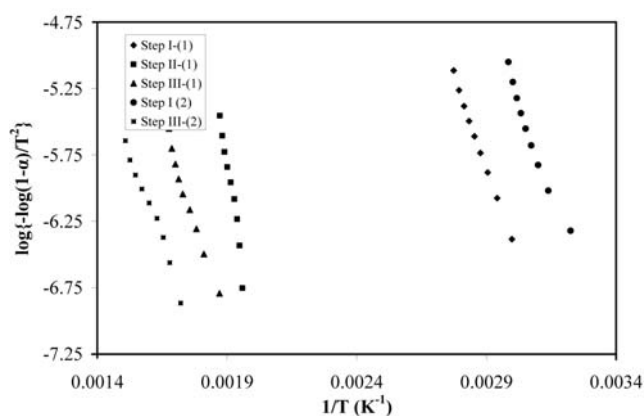


Fig. 6. Typical Coats–Redfern plot of the complexes

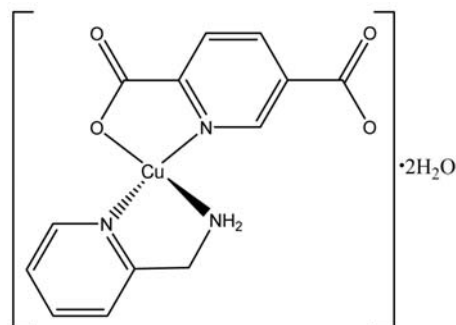


Fig. 7. Proposed structure for the  $[Cu(pydc)(2-amp)] \cdot 2H_2O$  (**1**)

### 3. 4. Biological Activity

The ligands and complexes have been evaluated in vitro against Gram-positive, Gram-negative bacteria and yeast and molds, which are known to cause infections in humans. The results of antimicrobial activity of the two ligands (8-HQ and 2-amp) and the two compounds ( $[Cu(pydc)(2-amp)] \cdot 2H_2O$  (**1**),  $[Cu(pydc)(8-HQ)] \cdot H_2O$  (**2**)) obtained by the disc diffusion method are presented in

Table 2. Thermodynamic parameters for thermal decomposition the complexes

Complex	Step	$E_a$ (kJ/mol)		$A$ ( $s^{-1}$ )		$r^2$		$\Delta H^\ddagger$ (kJ/mol)		$\Delta S^\ddagger$ (J/mol)		$\Delta G^\ddagger$ (kJ/mol)	
		C-R	H-M	C-R	H-M	C-R	H-M	C-R	H-M	C-R	H-M	C-R	H-M
(1)	I	106.66	119.43	$2.57 \times 10^{15}$	$4.95 \times 10^{15}$	0.999	0.999	103.69	116.46	48.59	54.04	86.31	97.13
	II	253.68	270.04	$6.99 \times 10^{24}$	$7.04 \times 10^{26}$	0.964	0.963	249.26	265.62	225.94	264.30	129.18	196.96
	III	117.20	109.14	$5.6 \times 10^{16}$	$9.67 \times 10^{16}$	0.983	0.991	112.56	104.25	70.07	74.62	71.31	60.32
(2)	I	101.49	99.28	$2.84 \times 10^{15}$	$4.10 \times 10^{15}$	0.973	0.974	98.71	96.50	49.99	53.04	82.02	78.78
	III	101.63	133.30	$1.36 \times 10^{14}$	$1.26 \times 10^{14}$	0.984	0.980	95.98	127.65	18.18	18.81	83.62	114.86

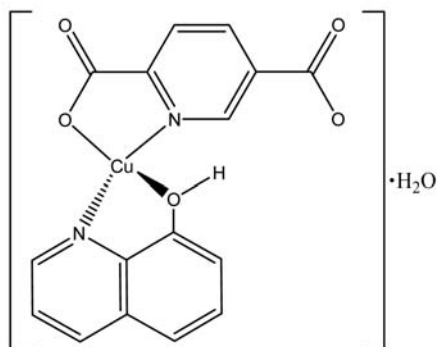
Fig. 8. Proposed structure for the  $[Cu(pydc)(8-HQ)] \cdot H_2O$  (2)

Table 3. Antimicrobial activity was determined for 100  $\mu\text{g}/\text{disc}$  and 200  $\mu\text{g}/\text{disc}$  concentrations against tested microorganisms. The comparative activity of currently used antibacterial agent tetracycline and antifungal agent nystatin are presented in Table 3. The 2-amp did not show antimicrobial activity against *B. cereus*, *P. vulgaris*, *R. rubra* and *A. niger* at 200  $\mu\text{g}/\text{disc}$  concentration. The 2-amp ligand show antimicrobial activity against *S. aureus*, *E. coli*, *E. aerogenes*, *S. epidermidis*, *N. canis*, *P. aeruginosa* and *C. albicans* with the diameters of zone inhibition ranging between 7–10 mm at 200  $\mu\text{g}/\text{disc}$  concentration. The compound **1** showed weak or absent antibacterial and antifungal activity against some of the tested Gram-positive, Gram-negative bacterial strains, yeast and fungi, with the diameters of zone inhibition ranging between 7–9 mm at 200  $\mu\text{g}/\text{disc}$  concentration. The compound **1** did not show antimicrobial activity against *E. aerogenes*, *P. aeruginosa*, *P. vulgaris* and *A. niger* at 200  $\mu\text{g}/\text{disc}$  concentration. The 2-amp and the compound **1** did not show antimicrobial activity against *P. vulgaris* and *A. niger* at the tested concentrations. The 8-HQ show good antimicrobial activity against all tested microorganisms. It showed antimicrobial activity against the tested Gram-positive, Gram-negative bacterial strains, yeast and fungi, with the 20–67 mm at 200  $\mu\text{g}/\text{disc}$  concentration. 8-Hydroxyquinoline (8-HQ) and its derivatives are well known for their antifungal, antibacterial and antiamoebic activities.<sup>45</sup> The 8HQ exhibited antimicrobial activity with 20 mm inhibition zone diameter against *P. vulgaris*

and the highest activity with 67 mm inhibition zone diameter against *S. aureus* at 200  $\mu\text{g}/\text{disc}$  concentration. The activity of the new synthesized complexes and ligands increases as the concentration increases. *S. aureus* was used due to its clinical relevance as a major cause of hospital acquired infections of surgical wounds and infections associated with in-dwelling medical devices. Besides, *S. aureus* rapidly develops resistance to many antimicrobial agents.<sup>46</sup> The 8-HQ ligand showed antifungal activity against *C. albicans*, *R. rubra* and *A. niger* again with the diameters of zone inhibition ranging between 57–60 mm in the same concentration.

The compound **2** showed antibacterial and antifungal activity against all or some of the tested Gram-positive, Gram-negative bacterial strains, yeast and fungi, with the diameters of zone inhibition ranging between 7–45 mm at 200  $\mu\text{g}/\text{disc}$  concentrations. Our findings show that the compound **2** has broad spectrum antimicrobial activity against Gram-positive, Gram-negative bacteria (except *E. aerogenes*), yeast and mold strains at the 200  $\mu\text{g}/\text{disc}$  concentration. Çolak et al.<sup>47</sup> found that  $(8-H_2Q)_2[Mn(dipic)_2] \cdot 6H_2O$  and  $(8-H_2Q)_2[Zn(dipic)_2] \cdot 6H_2O$  (dipic = pyridine-2,6-dicarboxylic acid) showed good inhibition effect against Gram-positive bacteria and fungi. The results obtained in this study are in good agreement with our earlier study.<sup>47</sup> The compound **2** did not show antibacterial activity against *E. aerogenes* but the 8-HQ show antibacterial activity with 38 mm inhibition zone diameter at 200  $\mu\text{g}/\text{disc}$  concentration. In classifying the antibacterial activity as Gram-positive or Gram-negative, it would generally be expected that a much greater number would be active against Gram-positive than Gram-negative bacteria.<sup>48</sup> The outer membrane of Gram-negative bacteria is the first barrier capable of limiting the penetration of antimicrobial agents. This fact is widely known and referred to as “intrinsic resistance” of Gram-negative bacteria.<sup>49</sup> Our results are in accordance with the literature. The 8-HQ ligand alone showed good antimicrobial activity inhibition zone 20–67 mm against all tested microorganisms. Complex **2** showed higher antimicrobial activity for microorganisms tested than complex **1**. This can be attributed to the presence of 8-HQ in the complex **2**. The complex **2** showed good antifungal activity inhibition zone 25–45 mm against *C. albicans*, *R. rubra* and *A. niger*. *C. albicans* is

one of the most pervasive pathogenic fungi, especially infecting immuno-compromised hosts, in which it can invade various tissues.<sup>46</sup> Rohde et al.<sup>50</sup> found that antibacterial activity of 8-hydroxyquinoline plus copper sulphate was markedly enhanced on Gram-positive bacteria like *S. aureus*. Leon et al.<sup>51</sup> found that copper sulphate combined with 8-hydroxyquinoline and copper sulphate alone were the most effective treatments in reducing symptoms in plants inoculated with *Clavibacter michiganensis* subsp. *michiganensis*. Substituted derivatives of 8-HQ are known inhibitors of catechol *O*-methyltransferase.<sup>52</sup> Daniel et al.<sup>52</sup> found that several copper compounds, such as NCI-109268 and bis-8-hydroxyquinoline copper(II) [Cu(8-HQ)<sub>2</sub>], can inhibit the chymotrypsin-like activity of purified 20S proteasome. Furthermore, proteasome inhibition and apoptosis induction were detected in prostate cancer cells treated with the ligand 8-HQ alone following pre-treatment with

copper(II) chloride.<sup>53</sup> In our study, microbial activities of the complexes against tested microorganisms are lower than that of standard antibiotics.

The minimum inhibitory concentrations (MIC) results of the compound **2** are presented in Table 4. MIC of the compound **2** for the microorganisms species mainly ranged from 1.95 to 15.6 µg/mL, and the lowest MIC values were found for the *C. albicans* and *A. niger*. From these result it is seen that the complex **2** demonstrates a low inhibiting ability toward Gram-negative bacteria (MIC: *P. vulgaris* 15.6, *P. aeruginosa* 7.8 µg/mL).

## 4. Conclusions

A new series of copper(II) complexes were synthesized and characterized by elemental analysis and spectroscopic studies. Thermal characteristics of complexes

**Table 3.** Antimicrobial activity of the **1**, **2** and ligands.

Test Microorganisms	2-amp		1		8-HQ		2		Tetracycline	Nystatin
	100 µg	200 µg	10 µg/disc	100 U/disc						
<b>Bacterial strains</b>										
<i>S. aureus</i>	7	8	–	7	57	67	20	25	38	
<i>B. cereus</i>	–	–	7	9	50	58	20	22	28	
<i>S. epidermidis</i>	7	10	–	7	60	65	15	20	15	
<i>N. canis</i>	8	10	–	7	50	55	20	28	14	
<i>E. coli</i>	–	7	–	7	26	34	–	7	25	
<i>E. aerogenes</i>	–	7	–	–	30	38	–	–	14	
<i>P. aeruginosa</i>	7	9	–	–	50	60	12	18	13	
<i>P. vulgaris</i>	–	–	–	–	12	20	9	12	15	
<b>Fungal strains</b>										
<i>C. albicans</i>	7	10	7	8	40	60	40	45		20
<i>R. rubra</i>	–	–	7	8	40	57	18	25		21
<i>A. niger</i>	–	–	–	–	50	60	25	30		22

–; No inhibition of zone. All the microorganisms were resistant to the control DMSO.

**Table 4.** Minimum inhibitory concentration (MIC) for the [Cu(pydc)(8-HQ)] · H<sub>2</sub>O (**2**) against microorganism strains

Test Microorganisms	MIC for <b>2</b> (µg/mL)
<b>Bacterial strains</b>	
<i>S. aureus</i>	3.9
<i>B. cereus</i>	3.9
<i>S. epidermidis</i>	3.9
<i>N. canis</i>	3.9
<i>E. coli</i>	NT
<i>E. aerogenes</i>	NT
<i>P. aeruginosa</i>	7.8
<i>P. vulgaris</i>	15.6
<b>Fungal strains</b>	
<i>C. albicans</i>	1.95
<i>R. rubra</i>	3.9
<i>A. niger</i>	1.95

NT: No tested

have been studied. The activation energy of decomposition for complexes **1** and **2** obtained from two well known methods are in good agreement with the calculated values. Antibacterial activity of complexes has also been studied. The observed variation in the activity of the complexes across the various classes of organisms studied may be attributable to the differences in cell wall and/or membrane construction Gram-positive bacteria, Gram-negative bacteria and yeast and mould. Although the compound **2** shows antimicrobial activity against all Gram-positive bacteria, yeast and fungi, it needs to be investigated further.

## 5. Acknowledgments

This work was supported by Dumlupınar University, project No 2007/14.

## 6. References

1. P. Sengupta, S. Ghosh, T. C. W. Mak, *Polyhedron* **2001**, *20*, 975–980.
2. E. J. Jung, U. K. Lee, B. K. Koo, *Inorg. Chim. Acta* **2008**, *361*, 2962–2966.
3. Z. B. Han, Y. Ma, Z. G. Sun, W. S. You, *Inorg. Chem. Commun.* **2006**, *9*, 844–847.
4. L. B. Wang, V. R. Pan, P. Y. Zhan, Y. L. Niu, G. O. Zhang, *Acta Crystallogr.* **2007**, *E63*, m204–m206.
5. X. M. Li, Y. L. Niu, Q. W. Wang, B. Liu, *Acta Crystallogr.* **2007**, *E63*, m487–m488.
6. L. Mao, Y. Wang, Y. Qi, M. Cao, C. Hu, *J. Mol. Struct.* **2004**, *688*, 197–201.
7. M. I. Devereux, M. McCann, V. Leon, V. McKee, R. J. Ball, *Polyhedron* **2002**, *21*, 1063–1071.
8. M. C. Gossel, A. N. Dwyer, M. B. Hursthouse, J. B. Orton, *Cryst. Eng. Commun.* **2007**, 207–210.
9. D. Ang, G. B. Deacon, P. C. Junk, D. R. Turner, *Polyhedron* **2007**, *26*, 385–391.
10. X. Wang, C. Qin, E. Wang, L. Xu, Z. Su, *J. Mol. Struct.* **2006**, *796*, 172–178.
11. X. Wang, C. Qin, E. Wang, Y. Li, N. Hao, C. Hu, L. Xu, *Inorg. Chem.* **2004**, *43*, 1850–1856.
12. C. G. Arena, G. Bruno, F. Faraone, *Dalton Trans.* **1991**, 1223–1226.
13. T. Brasey, R. Scopelliti, K. Severin, *Chem. Commun.* **2006**, 3308–3310.
14. Y. C. Liang, R. Cao, W. P. Su, M. C. Hong, W. J. Zhang, *Angew. Chem.* **2000**, *112*, 3442–3445; *Angew. Chem. Int. Ed.* **2000**, *39*, 3304–3307.
15. S. Takamaizawa, M. Furihata, S. Takeda, K. Yamaguchi, W. Mori, *Macromolecules* **2000**, *33*, 6222–6227.
16. D. W. Min, S. S. Yoon, D. Y. Jung, C. Y. Lee, Y. Kim, W. S. Han, S. W. Lee, *Inorg. Chim. Acta* **2001**, *324*, 293–299.
17. Y. C. Liang, M. C. Hong, W. P. Su, R. Cao, W. J. Zhang, *Inorg. Chem.* **2001**, *40*, 4574–4582.
18. C. Xie, B. Zhang, X. Wang, B. Yua, R. Wang, G. Shena, D. Shena *Z. Anorg. Allg. Chem.* **2008**, *634*, 387–391.
19. K. Y. Choi, K. M. Chun, I. H. Suh, *Polyhedron* **2001**, *20*, 57–65.
20. A. J. Lough, R. M. Gregson, G. Ferguson, C. Glidewell, *Acta Crystallogr.* **2000**, *B56*, 85–93.
21. M. J. Plater, M. R. S. J. Foreman, R. A. Howie, E. E. Lachowski, *J. Chem. Res(S)*. **1998**, 754–755.
22. G. Mendoza-Díaz, G. Rigotti, O. E. Piro, E. E. Sileo, *Polyhedron* **2005**, *24*, 777–783.
23. B. O. Patrick, C. L. Stevens, A. Storr, R. C. Thompson, *Polyhedron* **2005**, *24*, 2242–2249.
24. J. L. Lu, D. S. Zhang, L. Li, B. P. Liu, *Acta Crystallogr.* **2006**, *E62*, m3321–m3322.
25. L. Xue, F. Luo, Y. X. Che, J. M. Zheng, *J. Mol. Struct.* **2007**, *832*, 132–137.
26. H. Kumagai, H. Sobukawa, M. Kurmoo, *J. Mater. Sci.* **2008**, *43*, 2123–2130.
27. S. T. Chuang, F. M. Shen, T. S. Kuo, K. B. Shiu, *J. Chin. Chem. Soc.* **2007**, *54*, 893–902.
28. J. Y. Lu, V. Schauss, *Cryst. Eng. Comm.* **2002**, *4*, 623–625.
29. A. P. Singh, N. K. Kaushik, A. K. Verma, G. Hundal, R. Gupta, *Eur. J. Med. Chem.* **2009**, *44*, 1607–1614.
30. G. Nicoletti, E. Domalewska, R. Borland, *Mycol. Res.* **1999**, *103*, 1073–1084.
31. National Committee for Clinical Laboratory Standards. Performance standards for antimicrobial disk susceptibility Test-fourth Edition. Approved Standard NCCLS Document M2-A4, Vol: 10. No: 7. Villanova, **1990a**, P.A, 9–15.
32. National Committee for Clinical Laboratory Standard. Second Edition. Methods for dilution antimicrobial susceptibility tests for bacteria that grow aerobically. Approved Standard NCCLS Document M7-A2 Vol 10, No: 8, Villanova, **1999b**, P.A, 12–15.
33. National Committee for Clinical Laboratory Standards. Reference Method for broth dilution antifungal susceptibility testing of filamentous fungi. Approved Standard (M38-A). NCCLS Document M38-A. Vol: 22. No: 16, Villanova, **2002**, P.A.
34. H. L. Gao, C. Cheng, B. Ding, W. Shi, H. B. Song, P. Cheng, D. Z. Liao, S. P. Yan, Z. H. Jiang, *J. Mol. Struct.* **2005**, *738*, 105–111.
35. X. Haitao, Z. Nengwu, X. Hanhui, W. Yonggang, Y. Ruyi, Y. Enyi, J. Xianglin, *J. Mol. Struct.* **2001**, *597*, 1–5.
36. L. P. Sun, S. Y. Niu, J. Jin, G. D. Yang, L. Ye, *Eur. J. Inorg. Chem.* **2006**, *2006*, 5130–5137.
37. K. Nakamoto: *Infrared and Raman Spectra of Inorganic and Coordination Compounds*. 5th ed., Wiley Interscience, New York, **1997**, pp. 59–62.
38. L. Puntus, V. Zolin, V. Kudryashova, *J. Alloys and Comp.* **2004**, *374*, 330–334.
39. A. B. P. Lever, *Inorganic Electronic Spectroscopy*, Elsevier, New York, **1968**.
40. W. J. Geary, *Coord. Chem. Rev.* **1971**, *7*, 81–122.
41. H. Horowitz, G. Metzger, *Anal. Chem.* **1963**, *35*, 1464–1468.
42. A. W. Coats, J. P. Redfern, *Nature* **1964**, *201*, 68–69.
43. A. A. El-Sherif, B. J. A. Jeragh, *Spec. Acta Part A* **2007**, *68*, 877–882.
44. E. E. Sileo, G. Rigotti, B. E. Rivero, M. A. Blesa, *Phys. Chem. Solids* **1997**, *58*, 1127–1135.
45. K. Arıcı, M. Yurdakul, S. Yurdakul, *Spectrochimica Acta Part A* **2005**, *61*, 37–43.
46. D. Esquenazi, M. D. Wigg, M. M. F. S. Miranda, H. M. Rodrigues, J. B. F. Tostes, S. Rozental, A. J. R. da Silva, C. S. Alviano, *Res. Microbiol.* **2002**, *153*, 647–652.
47. A. T. Çolak, F. Çolak, O. Z. Yeşilel, O. Büyükgüngör, *J. Mol. Struct.* **2009**, *936*, 67–74.
48. A. R. M. Cutheon, S. M. Ellis, R. E. W. Hancock, G. H. N. Towers, *J. Ethnopharmacol.* **1992**, *37*, 213–223.
49. N. V. Loginova, T. V. Koval'chuk, R. A. Zheldakova, N. P. Osipovich, V. L. Sorokin, G. I. Polozov, G. A. Ksendzova, G. K. Glushonok, A. A. Chernyavskaya, O. I. Shadyro, *Bioorg. Med. Chem. Lett.* **2006**, *16*, 5403–5407.

50. W. Rohde, P. Mikelens, J. Jackson, J. Blackman, J. Whitcher, W. Levinson, *Antimicrob. Agents Chemother.* **1976**, *10*, 234–240.
51. R. Huang, A. Wallqvist, D. G. Covell, *Biochem. Pharmacol.* **2005**, *69*, 1009–1039.
52. K. G. Daniel, P. Gupta, R. H. Harbach, W. C. Guida, Q. P. Dou, *Biochem. Pharmacol.* **2004**, *67*, 1139–1151.
53. L. de León, F. Siverio, M. M. López, A. Rodríguez, *Crop Protection* **2008**, *27*, 1277–1283.

## Povzetek

Predstavljamo sintezo dveh kvadratno planarnih bakrovih(II) kompleksov: (2-aminometilpiridin-piridindikarboksilato)bakrovega(II) dihidrata,  $[\text{Cu}(\text{pydc})(2\text{-amp})] \cdot 2\text{H}_2\text{O}$  (**1**) in (8-hidroksikinolin-piridindikarboksilato)bakrovega(II) hidrata,  $[\text{Cu}(\text{pydc})(8\text{-HQ})] \cdot \text{H}_2\text{O}$  (**2**) (2-amp = 2-aminometilpiridin, 8-HQ = 8-hidroksikinolin,  $\text{H}_2\text{pydc}$  = piridin-2,5-dikarboksilna kislina ali isocinkomeronična kislina). Poleg tega predstavljamo tudi preliminarano študijo kinetične in biološke aktivnosti pripravljenih bakrovih kompleksov. Komplekse smo karakterizirali na osnovi elementne analize, s spektroskopskimi metodami (FT-IR, UV in masni spektri), s termično analizo in z meritvami magnetnostnih in prevodnostnih lastnosti. Kinetične parametre smo za vsako posamezno stopnjo termičnega razpada kompleksov dobili s pomočjo metod po Coats–Redfern in Horowitz–Metzger. Antimikrobne aktivnosti obeh kompleksov in dveh ligandov smo določili z metodo difuzije v agarju. Antimikrobna aktivnost kompleksa **2** je bila določena z metodo redčenja v agarju. Rezultate smo primerjali z rezultati za dva dobro znana antibiotika: tetraciklin in nistatin.